Scientia Iranica A (2011) 18 (4), 827–834

Sharif University of Technology

Scientia Iranica

Transactions A: Civil Engineering

www.sciencedirect.com

New modeling for moment–rotation behavior of bolted endplate connections

M.R. Mohamadi-Shoore [a], **M. Mofid** [b,*]

[a] *Department of Civil Engineering, Islamic Azad University, Chalus, Iran*

[b] *Department of Civil Engineering, Sharif University of Technology, Tehran, Iran*

Received 22 June 2008; revised 16 April 2011; accepted 13 June 2011

KEYWORDS

Moment-rotation curve;
Semi-rigid;
Endplate;
Bolted connection.

Abstract A new exponential model to depict the moment–rotation (M–θ) relationship of Bolted Endplate Connections (BEC) is proposed. The proposed model represents an approach to the prediction of M–θ curves, taking into account the possible failure modes and the deformation characteristics of the connection elements. The presented model has three physical parameters, along with two curve-fitted factors. These physical parameters are generated from dimensional details of the connection, as well as the material properties. By employing simplified connection behavioral models to estimate the connection M–θ behavior, analytical expressions for evaluating major connection parameters, such as initial stiffness and ultimate moment, are derived. The M–θ curves obtained by the model are compared with published connection tests and 3D FEM research. The model yields acceptable results in good agreement with actual connection behavior. Besides, comparison between the presented model and other existing equations, in prediction of the derived BEC's M–θ curve, shows the reasonably accurate results of the proposed model.

1. Introduction

Beam-to-column connections often significantly influence the behavior of steel building frames. The connection deformation, in combination with the P–Δ effect, easily leads to excessive lateral drift in the unbraced multistory frames. In the braced frames, beam-to-column connections that have been assumed to act as "pins" may transmit significant flexural moments from the beams to the columns. While in some cases, the moments may enhance column stability, in several other cases, it may not be conservative to ignore it in the design [1]. Moreover, evaluation of the ultimate strength capacity, the initial stiffness of the M–θ curve, and the ultimate rotation capacity of the connections can all straightforwardly be assessed directly from the connections' M–θ curve [2]. Recently, numerous studies have proposed parametric studies with various models to represent M–θ behavior for some different types of beam-to-column and beam-to-beam connections [3–16]. Only a few of these models adequately come close to characterizing some special M–θ behavior through the full range of loading/rotations [17]. Due to the sensitivity of the connection performance, with respect to the different configuration and/or material properties, the results do not get well fitted into the experimental test curves [5]. In addition, the procedures have been able to employ only one type of connection; therefore, the course of actions must be repeated for all different connection types. As it would be excessively expensive to store the M–θ relationships for all practical connection types and sizes, a feasible solution is to derive and store a single "standardized" M–θ function for each connection type.

In this paper, a new exponential model is developed to predict the standard M–θ curve of BEC by determining initial stiffness, strain hardening stiffness, the intercept constant moment and two curve-fitness parameters. The presented exponential model is used to represent the entire M–θ behavior of the BEC. The major parameters of this "standard M–θ utility" will be obtained based on theoretical methods.

2. Modeling functions

There are different studies that have proposed various models to represent the non-linear M–θ behavior of the connections [3–16]. The functions of these different models are written

* Corresponding author.
E-mail address: mofid@sharif.edu (M. Mofid).

doi:10.1016/j.scient.2011.07.015

Nomenclature

$A_{s\text{-bolt}}, E_{\text{bolt}}, \sigma_{y\text{-bolt}}, d_{\text{bolt}}, n$ Bolt net area, modulus of elasticity, yield stress, diameter and number of bolts in each raw respectively

$A_f, A_w, h_b, d_b, b_{fb}, t_{wb}, t_{fb}, t_{wb}, I_b, z_b, \sigma_{yb}$ Beam section flange area, web area, height, depth, flange width, web thickness, flange thickness, inertia moment, plastic modulus and yield stress, respectively

$A_c, A_{cv}, h_c, d_c, b_{fc}, t_{wc}, t_{fc}, k_{c1}, I_c, z_c, \sigma_{yc}$ Column section area, shear area, height, depth, flange width, web thickness, flange thickness, flange root radius, inertia moment, plastic modulus and yield stress, respectively

$a^*, \ell_p, \lambda_e, Q, R_o, R_1, R_2, R_3, R_4, R_5$ Coefficients defined in Table 2

$M_u, M_{ue}, M_{uf}, M_{uw}, M_{ub}, M_{usc}$ Ultimate moment applied to connection, end plate, column flange, column web, bolts and beam and column sections, respectively

b, d_e, g, P_{fi}, P_t Geometry parameters of connection, shown in Figure 2

b_p, t_p, σ_{yp} Endplate width, thickness and yield stress, respectively

E Young's modulus of elasticity

F Beam flange force

K_i Initial stiffness of the connection

K_p Strain hardening stiffness of the connection

M, M_y, M_o Moment (general), yielding moment and intercept-constant moment, respectively

T Force in beam tension flange

$\theta, \theta_y, \theta_u$ Rotation (general), yielding rotation and ultimate rotation, respectively

λ Coefficient defined in Table 3

σ_y Yield stress of material

ν Poisson's ratio

in Table 1. Only a few of these models adequately come close to characterizing some special M–θ behavior through the full range of loading/rotations [18]. Chen et al. [5] show that due to the inherent oscillatory nature of the polynomial series, they may yield erratic tangent stiffness values. Furthermore, in these polynomial series functions, the implicated parameters usually have very little physical meaning. Due to their nature, the simplest form of power model does not represent the connection behavior adequately. It is unsuitable if accurate results are desired [17]. The M–θ curves of some connections, such as BEC, do not flatten out near the state of ultimate strength of the connection. This means that the plastic stiffness (strain hardening stiffness) of these connections will not be zero. Thus, most functions of Table 1, including Nos. 4, 5, 6, 7, 8 and 13 are unsuitable for this type of connection. While the multi-parameter exponential models (Lui–Chen function [12] and Kishi–Chen function [13]) can provide a good fit, they involve a large number of parameters. Therefore, a large number of data are required in their curve-fitting process; this fact makes their practical use difficult.

In spite of the fact that the Chisala exponential function [16] has all above mentioned required conditions, this model does not have a shape parameter. Therefore, this model does not represent the connection behavior adequately [19]. The remaining models, including the Richard–Hisa power model [11] and the

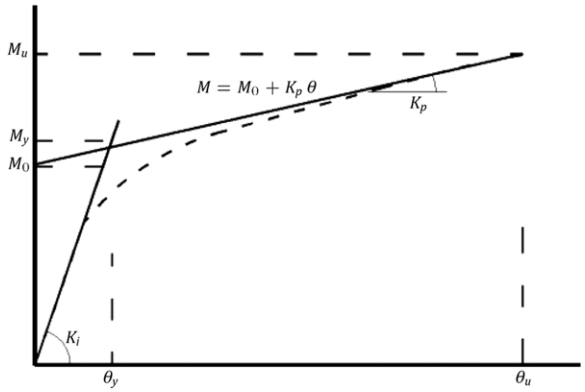

Figure 1: Typical form of M–θ curve.

Yee–Melcher exponential model [14], provide a proper fit and satisfy all previous mentioned required conditions. However, they are not presented in normalized form. In other words, their curve-fitness parameter is related to the dimension of other parameters. This restriction has limited the application of the model. Thus, the new normalized M–θ model is derived in this paper.

3. Analytical study

By considering the conditions of a rigid connection general M–θ curve, a model function should satisfy evidently the following boundary conditions:

1. The M–θ curve should be passed through the origin: $M|_{(\theta=0)} = 0$.
2. The M–θ curve should be passed through the ultimate point: $M|_{(\theta=\theta_u)} = M_u$.
3. The slope of the M–θ curve at the origin is equal to the initial stiffness: $\frac{dM}{d\theta}\Big|_{(\theta=0)} = K_i$.
4. As the rotation becomes large ($\theta \longrightarrow \theta_u$), the M–θ curve tends to the straight line, represented by $M = M_o + K_p\theta$, where M_o is defined as the normalizing moment or the intercept constant moment and K_p is the strain hardening stiffness of the M–θ curve in the plastic zone, as shown in Figure 1.

In addition to above mentioned boundary conditions, the model function must have the ability to correlate with experimental results. Based on the current knowledge of connection behavior and modeling requirements, a proper model should be adopted.

Mohamadi [17] showed a simple exponential function that satisfies the above mentioned requirements, having the following general form of:

$$M = (a_1 + a_2\theta)\left(1 - e^{(-a_3(1+a_4\theta)\theta)}\right) + a_5\theta, \tag{1}$$

where a_1, a_2, a_3, a_4 and a_5 are the model parameters, which can be obtained as follows:

For all values of model parameters, the first boundary condition is satisfied. Differentiating Eq. (1) and substituting for $\theta = 0$ yields:

$$\frac{dM}{d\theta}\bigg|_{(\theta=0)} = a_1a_3 + a_5 = K_i. \tag{2}$$

For satisfying the third boundary condition, it can be written:

$$\text{Lim}\frac{dM}{d\theta}\bigg|_{(\theta\to\infty)} = a_2 + a_5 = K_p. \tag{3}$$

Table 1: Different M–θ models.

Type	Name	Function	ID no.
Polynomial model	Frye–Morris function [3]	$\theta = C_1(KM)^1 + C_2(KM)^3 + C_3(KM)^5$	1
	Picard–Giroux function [4]	$\theta = C_1(KM)^1 - C_2(KM)^2 + C_3(KM)^5$	2
Power model	Simplest form of power model [5]	$\theta = aM^b$	3
	Ramberg–Osgood function [6]	$\theta = \frac{M}{K_i}\left(1 + K(M/K_i)^{n-1}\right)$	4
	Ang–Morris function [7]	$\frac{\theta}{\theta_o} = \frac{M}{M_o}\left(1 + (M/M_o)^{n-1}\right)$	5
	Richard–Abbutt function [8]	$M = \frac{K_i\theta}{[1+(K_i\theta/M_u)^n]^{1/n}}$	6
	Colson–Louveau function [9]	$\theta = \frac{M}{K_i}\cdot\frac{1}{1-(M/M_u)^n}$	7
	Kishi–Chen function [10]	$\theta = \frac{M}{K_i}\cdot\frac{1}{[1-(M/M_u)^n]^{1/n}}$	8
	Richard–Hisa function [11]	$M = \frac{(K_i-K_p)\theta}{[1+[(K_i-K_p)\theta/M_u]^n]^{1/n}} + K_p\theta$	9
Exponential model	Lui–Chen function [12]	$M = \sum_{j=1}^{m} C_j\left(1 - \exp\left(-\theta/2j\alpha\right)\right) + M_o + K_p\theta$	10
	Kishi–Chen function [13]	$M = \sum_{j=1}^{m} C_j\left(1 - \exp\left(-\theta/2j\alpha\right)\right) + M_o + \sum_{k=1}^{n} C_k\left(\theta - \theta_k\right)H\left(\theta - \theta_k\right)$	11
	Yee–Melcher function [14]	$M = M_u\left(1 - \exp\left(-(K_i - K_p + C\theta)\theta/M_u\right)\right) + K_p\theta$	12
	Wu–Chen function [15]	$\frac{M}{M_u} = n\left(\ln\left(1 + K_i\theta/M_u\right)\right)$	13
	Chisala function [16]	$M = \left(M_o + K_p\theta\right)\left(1 - \exp\left(-K_i\theta/M_o\right)\right)$	14

According to the fourth boundary condition, when rotation (θ) becomes large, the M–θ curve tends to the straight line, therefore:

$$\lim_{(\theta\to\infty)} M = a_1 + (a_2 + a_5)\theta = M_o + K_p\theta. \quad (4)$$

Therefore, parameter a_1 represents the intercept constant moment, M_o. If parameters, a_4 and a_5, are replaced by β and αK_p, the other parameters are yielded and the function of the model is expressed as follows:

$$M = \alpha K_p\theta + (M_o + (1-\alpha)K_p\theta)\left(1 - e^{\left(\frac{-(K_i-\alpha K_p)(1+\beta\theta)\theta}{M_o}\right)}\right), \quad (5)$$

where M_o is the intercept constant moment, K_i is the initial stiffness, K_p is the strain hardening stiffness and finally α and β are the shape parameters obtained from calibration with the experimental data. The parameter, β, is introduced to manage the rate of decay of the slope of the curve. Moreover, K_p can be substituted as follows:

$$K_p = \frac{M_y - M_o}{\theta_y}. \quad (6)$$

Then, substituting Eq. (6) into Eq. (5), the following dimensionless form of the Mohamadi function gives us:

$$\frac{M}{M_o} = \alpha m^*\frac{\theta}{\theta_y} + \left(1 + (1-\alpha)m^*\frac{\theta}{\theta_y}\right)\left(1 - e^{-\left(1+\beta\frac{\theta}{\theta_y}\right)\frac{\theta}{\theta_y}}\right), \quad (7)$$

where m^* is defined as $\left(\frac{M_y}{M_o} - 1\right)$. It is worthy to note that with respect to the Mohamadi function [17], when shape parameters are assumed to be zero, the Chisala exponential function [16] is obtained. Mohamadi [17], through a parametric study, obtained the appropriate values of α and β for BEC as 1.0 and zero, respectively. Then, the Mohamadi function for BEC is expressed as follows:

$$\frac{M}{M_o} = \left(1 - e^{-\frac{\theta}{\theta_y}}\right) + \left(\frac{M_y}{M_o} - 1\right)\frac{\theta}{\theta_y} \quad \therefore 0 \le \theta \le \theta_u. \quad (8)$$

In order to utilize this model for any connections, the corresponding parameters must be calculated. The three physical parameters can be derived through analytical procedures, as well as numerical parametric studies. In spite of the fact that there are two shape parameters in the presented function, the accuracy of the predicted curve is extremely affected by the precision of prediction of the physical parameters, which are evaluated as described in the sections to follow.

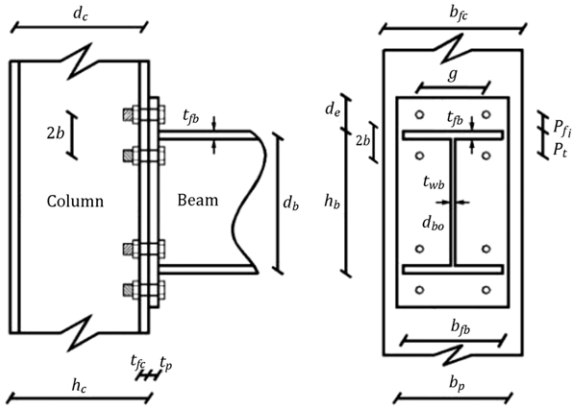

Figure 2: Extended end plate connection.

4. Evaluation of the model parameters

In order to demonstrate the capability of the proposed model in representing the M–θ behavior of BEC, the presented model was fitted to some connection test data obtained from literature. To this purpose, more than seventy investigations simulating BEC M–θ behavior, along with representing the connection properties such as ultimate moment, were listed and studied in [17]. However, only a few of these studies come close to adequately characterizing the connection initial stiffness, strain hardening stiffness and other properties of the connection's M–θ behavior. Based upon these studies, a typical BEC, which is shown in Figure 2, is selected and analytical expressions for evaluating the presented model parameters, K_i, K_p and M_o, are derived in the sections to follow. It is to note that the stress–strain relationship for the endplate, column and beam is taken as an elastic perfectly plastic model, as shown in Figure 3.

4.1. Evaluation of initial stiffness, K_i

For evaluating stiffness properties, such as initial stiffness, most of these analytical studies have used component methods [17,20]. In the context of the component method, whereby a joint is modeled as an assembly of springs (components) and rigid links, using an elastic post-buckling analogy to the bilinear elastic–plastic behavior of the each component, a general

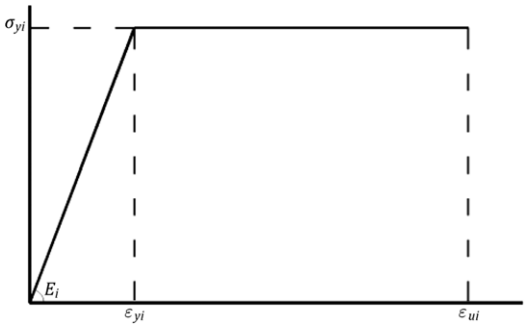

Figure 3: Idealized steel stress–strain curve.

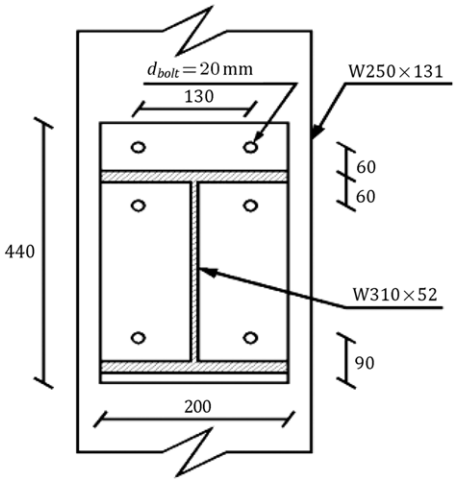

Figure 4: Example problem end plate with various thicknesses (12, 15, 20 and 25 mm).

analytical model is proposed that yields the initial stiffness and the strain hardening stiffness of the connection. Consequently, the rotational stiffness of a connection is directly related to the deformation of the individual connection elements. Generally, the behavior of the connection largely depends on the component behavior of the tension zone the compression zone, and the shear zone. The basic components, which contribute to the deformation of the common BEC, are identified as: (1) endplate, (2) pretension bolts, (3) column flange, and (4) column web. The EC3 [20] propose components methods for modeling basic components as equivalent T-stub flanges. Moreover, Mohamadi and Mofid [21] suggested a general expression for initial stiffness, K_i, formulated in Table 1, which shows the expressions for the initial stiffness of BEC in detail.

4.2. Evaluation of intercept constant moment

The intercept constant moment, M_o, is selected as the moment corresponding to the intersection of the moment axis and the strain hardening tangent stiffness line, which passes through the ultimate point, as shown in Figure 1. Therefore, the intercept constant moment is highly dependent on the connection ultimate moment. For determination of the intercept-constant in this paper, the ultimate moment is firstly evaluated. The different components contributing to the overall response of generic BEC are:

1. Column web in shear, compression and tension.
2. Column flange in bending.
3. Endplate in bending.
4. Bolts in tension and shear.
5. Beam flange and beam web in tension and compression.

On the basis of these assumptions, the moment capacity of BEC depends on the strength of the individual connection elements. Various investigations have shown that BEC will begin to lose its ability to sustain further loading when one or more of the following failure modes occur [22]:

1. Failure of bolts in the tension zone.
2. Yielding of the endplate in the tension zone and formation of the plastic mechanism.
3. Formation of the column flange plastic mechanism.
4. Shear yielding, buckling, or crippling of the column web.

These failure modes must be considered in terms of the moment acting on the connection. For this purpose, each of the aforementioned failure modes has been considered in terms of the tension or compression beam flange forces. Once the force in the beam flange has been determined, the capacity of the connection corresponding to each of the possible failure modes will be considered in terms of the flange force. Mohamadi et al. [23] have determined the ultimate force corresponding to each aforementioned component (endplate, tension bolts, column flange and column web). Thus, the lowest ultimate force value will present the amount of connection ultimate moment. The endplate and column flange bending behavior is similar to the beam bending behavior with a rectangular section. This kind of behavior, at bending loading, was demonstrated in many tests [19]. Based on this fact, the intercept-constant, M_o, can approximately be evaluated as a portion of the connection component ultimate moment [23]. Besides, Table 3 summarizes the equations used to evaluate M_o for BEC. The details regarding these equations are presented in [23].

4.3. Evaluation of strain hardening stiffness

Although there are different well-accurate methods for determination of the initial stiffness and strength of beam-to-column joints [23], there are no generally accepted analytical procedures for determination of the strain hardening stiffness, K_p. Indicatively, it may be said that the relevant Eurocode [20], as well as the AISC [24], do not propose any methods to determine the strain hardening stiffness. Likewise, there is no exact applicable analytical method for calculation of the strain hardening stiffness of the connections and usually test results are used to estimate its value. Empirically, after formation of plastic hinges in the connection components, the connection deformation can be calculated using the tangent modulus of elements [19]. Yee and Melchers [14] suggested that as strain hardening occurs subsequent to yielding, the shear modulus of the column web may be assumed to be approximated by 4% of the elastic shear modulus of the column, and also the strain hardening modulus can be adopted by 2% of the elastic modulus. Shi et al. [25] recommended that if the bolt tension stress reaches its yield stress, the tangent modulus of the bolt can be taken as 5% of the elastic modulus of the bolt. Besides, some studies have statistically inspected the ratio of K_p/K_i. For the BEC, Bahaari and Sherbourne [26] reported that a properly designed connection possesses a ratio of K_p/K_i; about or below 5%–3%. In addition, Mohamadi-Shoore and Mofid [21] have shown that the mentioned ratio corresponds to the connections failure mode. Based upon their results, if the column web failure

Table 2: Expressions for initial stiffness, K_i.

$$K_i = \frac{E.b.h_b^2}{(1-\lambda_e)\left(\frac{1}{K_o}+\frac{1}{2nK_3}+\frac{1}{K_4}+\frac{1}{K_5}\right)+\frac{6\lambda_e}{K_2}\left(\frac{K_2}{K_1}+\frac{1}{K_3}+\frac{1}{K_4}+\frac{2}{K_5}\right)},\ \lambda_e = \frac{t_{wb}/b_{fb}}{\frac{t_{wb}}{b_{fb}}+6\frac{t_{fb}}{d_{wb}}+2\frac{t_{fb}^3}{d_{wb}^3}}$$

$$R_o = \frac{t_p^3 b_p/b^2}{0.455b^2+1.56t_p^2},\ R_1 = \frac{8}{21(1-\nu^2)}\times\frac{Q.t_p^3/g}{7g^2+6t_p^2\left(8+\frac{g^2}{b^2}+\frac{g^2}{d_b^2}\right)},\ R_2 = \frac{64}{147}\frac{Q.b^2/d_b}{13d_b+16b-\frac{g^4}{b^3}}$$

$$R_3 = \frac{\frac{\pi}{4}b}{t_p+t_{fc}+1.2d_{\text{bolt}}+1.2}\left(1.33d_{\text{bolt}}+\frac{1}{2}\times\frac{t_p.t_{fc}}{t_p+t_{fc}}\right)^2,\ R_4 = \frac{4a^*.t_{fc}^3/\ell_p^3}{b+3.12bt_{fc}^2/\ell_p^2},\ R_5 = \frac{768I_c/b}{a^{*3}+16d_b^3}$$

$$Q = 208\left(1+\frac{h_b}{b}\right)+33.6\times\frac{g^2}{b^2}\left(1+\frac{b}{h_b}\right)+13\times\frac{g^4}{b^4}\left(1+\frac{b^3}{h_b^3}\right),\ \ell_p = g-t_{wc}-1.33d_{\text{bolt}}-t_p,\ a^* = 2\times b+g$$

Table 3: Considered mechanisms to calculate the ultimate moment, M_u.

$$\lambda = 1+\frac{A_w}{4A_f},\ \beta = \sqrt{\frac{2P_{fi}}{g}}+\sqrt{\frac{b_p}{2P_{fi}}},\ F_{\text{bolt}} = A_{s\text{-bolt}}\sigma_{y\text{-bolt}},\ \alpha_{ue_1} = \frac{b_p}{P_{fi}}+2\frac{d_b-P_t}{g-t_{wb}}+\frac{g-t_{wb}}{4d_b}$$

$$\alpha_{ue_2} = \frac{g+b_p}{4d_b}+\frac{d_b b_p}{4d_e d_b}+\beta^2\frac{P_{fi}}{d_b}+2\frac{F_{\text{bolt}}}{\sigma_{yp}t_p^2}\left(2-\frac{P_{fi}}{d_e}-\frac{P_t}{d_b}\right)$$

Endplate ultimate moment: $M_{ue} = \min\left(\alpha_{ue_1}, \alpha_{ue_2}\right)\times\lambda d_b\sigma_{yp}t_p^2$

Column flange ultimate moment: $M_{uf} = \min\left(\pi+\frac{2b}{b_{fc}-2k_{c1}}+\frac{4F_{\text{bolt}}}{\sigma_{yc}t_{fc}^2}\frac{b_{fc}-g}{b_{fc}-2k_{c1}}, \pi+2\frac{b_{fc}-g+2b-d_{bo}}{g-2k_{c1}}\right)\times\lambda d_b\sigma_{yc}t_{fc}^2$

Column web ultimate moment: $M_{uw} = \min\left(\frac{1}{\sqrt{3}}, \frac{t_{bf}+2t_p+5k_c}{d_{wc}}, \frac{10.765}{\sqrt{\sigma_{yc}}}\frac{t_{wc}^2}{(h_c-2k_c)d_{wc}}\right)\times\lambda\sigma_{yc}t_{wc}d_{wc}d_b$

Tension bolts ultimate moment: $M_{ubo} = 3\lambda d_b F_{\text{bolt}}$

Beam and column ultimate moment: $M_{us} = \min(\sigma_{yb}z_b, \sigma_{yc}z_c)$

Intercept-constant: $M_o = 0.75\times\min(M_{ue}, M_{uf}, M_{uw}, M_{ubo}, 1.07M_{us})$

Table 4: Required parameters of example problem.

t_p (mm)	K_i (kN m/mRad)	M_u (kN m)	M_o (kN m)	K_p/K_i (%)	K_p (kN m/mRad)
12	34.93	127	96	5	1.75
15	56.91	199	149	5	2.85
20	94.83	205	164	5	4.74
25	130.02	205	164	5	6.50

mode occurs, then the ratio of K_p/K_i may be assumed to be approximated by 3%; else, it can be considered as 5%.

5. Verifications

In order to evaluate the reliability of the presented exponential model, test results of two experimental and FEM studies are used for direct comparison. First, the Jenkins experimental program, which is represented in [19], was used for comparison with the delivered results. Based upon this experimental program, a BEC shown on Figure 4 with different thicknesses of 12 through 25 mm is considered. The corresponding parameters of the presented model are calculated accordingly and are shown in Table 4.

To demonstrate the ability of the proposed model, the corresponding curves, based upon the proposed model, have been achieved. In addition, a comprehensive comparison of the modeling results with the Jenkins experimental data and other existing predicting functions is carried out. The obtained M–θ curves corresponding to each function are shown in Figure 5. The involved function are: the exponential model of Yee and Melchers [14], the exponential model of Bahaari and Sherbourne [26], the polynomial model of Frye and Moris [3], the power model of Krishnamurthy et al. [27] and the power model of Tarpy and Cardinal [28]. In addition, the amount of beam ultimate moment (M_{us}) is determined for each figure. Secondly, to quantify the relative accuracy of the presented analytical model, along with considering various combinations of beams and columns in terms of load carrying capacity, eight connections that have been modeled exactly by Bahaari and Sherbourne [26] are selected. The corresponding properties, including endplate, beam and column, are shown in Tables 5 and 6, respectively. The modulus of elasticity of all components is considered as 210×10^9 N/m^2. Using the presented analytical method, the required parameters for each specimen are listed in Table 7. Finally, comparisons of the results with the aforementioned existing prediction methods are shown in Figures 5 and 6.

6. Summary and conclusion

In this study, a new exponential model capable of a complete demonstration of the M–θ relationship of the BEC has been outlined. Three physical parameters are required in this

Table 5: Schedule of different test problems, beam, column, end plate and bolts properties.

Ref.	No	Name	Beam section	σ_{yb} (MPa)	Column section	σ_{yc} (MPa)	b_p (mm)	d_e (mm)	b (mm)	g (mm)	d_{bolt} (mm)	P_{fi} (mm)	P_t (mm)	t_p (mm)	σ_{yb} (MPa)	$\sigma_{y\text{bolt}}$ (MPa)
Bahaari and Sherbourne [26]	1	PAR3e	W410*54	300	W200*100	300	210	126	72	120	24	59.8	83.2	30	300	627
	2	PPAR3e	W410*54	300	W200*100	300	210	126	72	120	24	59.8	83.2	24	300	627
	3	PAR4	W410*54	300	W200*100	300	210	126	72	120	24	59.8	83.2	15	300	627
	4	PAR10	W410*54	300	W200*100	300	210	126	72	120	24	59.8	83.2	40	300	627
	5	ION3	W610*82	250	W360*72	250	204	90	54	140	25.4	41.7	65.9	22	250	802
	6	ION3a	W610*82	250	W360*72	250	204	90	54	102	25.4	41.7	65.9	22	250	802
	7	PM7	W460*68	250	W250*73	250	194	124	68	120	24	53.0	82.2	15	250	627
	8	PAR1Ue	W410*54	300	W200*46	300	203	126	72	120	24	59.8	83.2	24	300	627

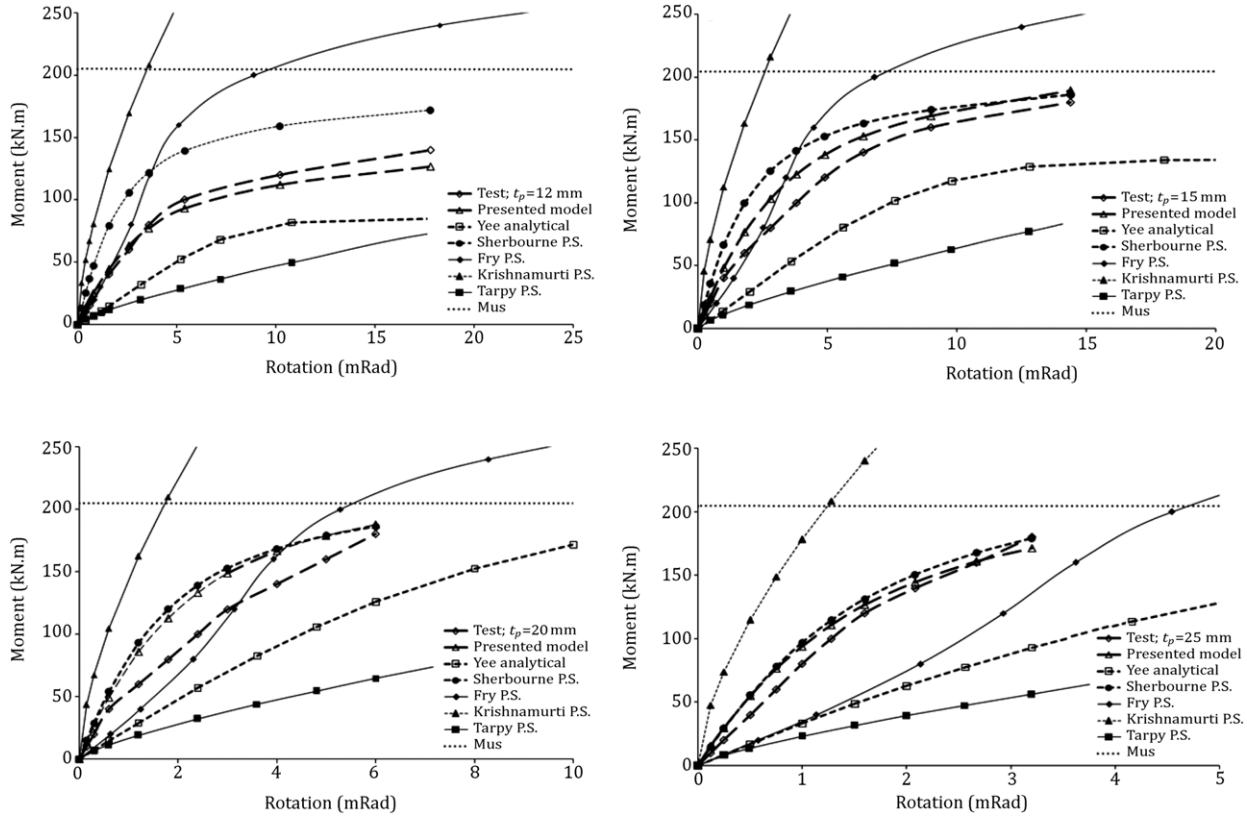

Figure 5: Comparison of M–θ curves between Jenkins tests and results of the various models.

Table 6: Dimensions of beams and columns used in this study.

Beam size	h_b (mm)	d_b (mm)	b_{fb} (mm)	t_{wb} (mm)	t_{fb} (mm)	z_b (mm^3)	k_{cl} (mm)	Column size	h_c (mm)	d_c (mm)	b_{fc} (mm)	t_{wc} (mm)	t_{fc} (mm)	A_c (mm^2)	I_c (mm^4)	z_c (mm^3)	k_c (mm)	k_{cl} (mm)
W310*52	318	304	167	7.6	13.2	8.39E5	14.3	W200*46	203	192	203	7.0	11.0	5 890	4.55E7	4.96E5	23.8	14.3
W460*52	450	439	152	7.8	11.0	1.09E6	19.1	W200*100	229	205	210	14.4	24.0	12 710	1.13E8	1.15E6	36.5	17.5
W410*54	403	392	177	7.8	11.0	1.05E6	19.1	W250*73	253	239	254	8.8	14.1	9 290	1.13E8	9.85E5	30.2	17.5
W460*68	459	444	154	9.1	15.2	1.49E6	20.6	W250*131	275	250	261	15.4	25.4	16 710	2.22E8	1.85E6	33.3	20.6
W610*82	599	586	178	10.0	12.9	2.20E6	23.8	W360*72	350	335	204	8.8	15.0	9 097	2.01E8	1.28E6	34.9	22.2

Table 7: Required parameters of specimens.

No.	K_i (kN m/mRad)	M_u (kN m)	M_o (kN m)	K_p/K_i (%)	K_p (kN m/mRad)
1	184.67	315	247.5	3	5.54
2	150.27	315	247.5	3	4.51
3	72.45	315	247.5	3	2.17
4	216.72	315	247.5	3	6.50
5	157.96	320	253.3	5	7.90
6	196.67	320	256.0	5	9.83
7	75.93	243	182.1	3	2.28
8	83.20	149	113.1	5	4.16

proposed model, which include 'the intercept-constant moment', 'the initial stiffness' and 'the strain hardening stiffness' of the connection. The first two parameters were analytically predicted from the geometry of the connection. Furthermore, the strain hardening (plastic) rotational stiffness parameter was approximately evaluated through simplified connection behavioral models. Moreover, these major parameters are employed in a presented exponential model for predicting the M–θ behavior of the BEC. In addition, several existing functions for modeling M–θ behavior have already been proposed in the literature. Likewise, several existing prediction equations particularly related to BEC have already been presented in the paper. Finally, the presented exponential model is applied to the M–θ data for a set of fourteen different BEC, which include four experimental tests and ten 3D FEM tests conducted by Bahaari et al. [26]. To demonstrate the accuracy of the proposed exponential model in comparison with other existing methods, the curves resulted from other existing prediction equations have been represented. A comparison of the results with experimental data, as well as finite element models, reveals very good agreement between them. Therefore, it was found to provide reasonably accurate approximations to the moment–rotation relationships for endplate connections. As a general conclusion, it can be stated that the procedures proposed in this paper provide the best prediction for evaluation of M–θ curves among mentioned prediction equations.

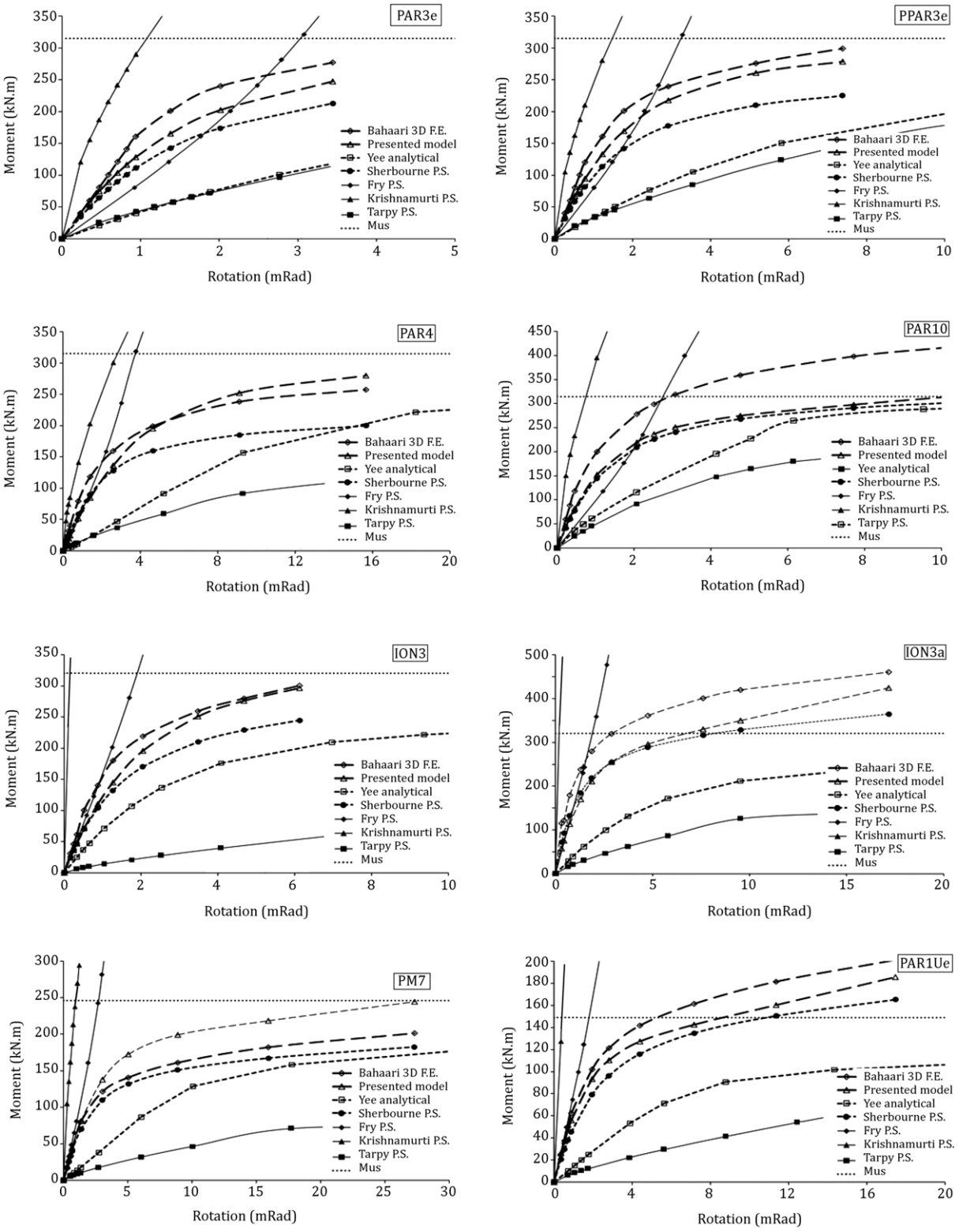

Figure 6: Comparison of M–θ curves between Bahaari 3D F.E. and results of the various models.

References

[1] Sherbourne, N.A. and Bahaari, M.R. "Finite element prediction of end plate bolted connection behavior. I: parametric study", *Journal of Structural Engineering, ASCE*, 123(2), pp. 157–164 (1997).

[2] Hashemi, M.J. and Mofid, M. "Evaluation of energy-based modal pushover analysis in reinforced concrete frames, with elevation irregularity", *Scientia Iranica*, 17(2), pp. 96–106 (2010).

[3] Frye, M.J. and Morris, G.A. "Analysis of flexibility connected steel frames", *Canadian Journal of Civil Engineering*, 2(3), pp. 280–291 (1975).

[4] Picard, A., Giroux, Y.M. and Brun, P. "Discussion of analysis of flexibly connected steel frames", *Canadian Journal of Civil Engineering, by Frye, M.J. and Morris, G.A.*, 3(2), pp. 350–352 (1976).
[5] Chen, W.F., et al. "Semi-rigid connections in steel frames", *Proc. Council on Tall Buildings and Urban Habitat*, McGraw-Hill, Inc., New York, NY (1993).
[6] Ramberg, W. and Osgood, W.R. "Description of stress–strain curves by three parameters", Technical Note No. 902, National Advisory Committee for Aeronautics, Washington, DC (1943).
[7] Ang, K.M. and Morris, G.A. "Analysis of three dimensional frames with flexible beam–column connections", *Canadian Journal of Civil Engineering*, 11, pp. 245–254 (1984).
[8] Richard, R.M. and Abbutt, B.J. "Versatile elastic–plastic stress–strain formula", *Journal of the Engineering Mechanics Division, ASCE*, 101(4), pp. 511–515 (1975).
[9] Colson, A. and Louveau, J.M. "Connection incidence on the inelastic behavior of steel structures", *Euromech Colloquium*, 174, (1983).
[10] Kishi, N. and Chen, W.F. "Moment-rotation relations of semi-rigid connections with angles", *Journal of Structural Engineering, ASCE*, 116(7), pp. 1813–1834 (1990).
[11] Richard, R.M., Hisa, W.K. and Chrnielowiec, M. "Derived moment–rotation curves for double framing angles", *Journal of Computers & Structures*, 30(3), pp. 485–494 (1998).
[12] Lui, E.M. and Chen, W.F. "Analysis and behavior of flexibly-jointed frames", *Engineering Structures*, 8, pp. 107–118 (1986).
[13] Kishi, N. and Chen, W.F. "Data base of steel beam to column connections", *Structural Engineering Report No. CE-STR-86-26, School of Civil Engineering*, Purdue University, West Lafayette, IN, 1986, p. 653.
[14] Yee, Y.L. and Melchers, R.E. "Moment-rotation curves for bolted connections", *Journal of Structural Engineering, ASCE*, 112(3), pp. 615–635 (1986).
[15] Wu, F.S. and Chen, W.F. "A design model for semi-rigid connections", *Engineering Structures*, 12(2), pp. 88–97 (1990).
[16] Chisala, M.L. "Modeling *M–f* curves for standard beam to column connections", *Engineering Structures*, 21(2), pp. 1066–1075 (1999).
[17] Mohamadi Shoore, M.R. "Parametric analysis on nonlinear behavior of bolted end plate connection", Sharif Univ. of Tech., Tehran, Iran, in Partial Fulfillment of the Requirements for Ph.D. Degree (2008).
[18] Riahi, A. and Curran, J.H. "Comparison of the cosserat continuum approach with the finite element interface models in the simulation of layered materials", *Scientia Iranica*, 17(1), pp. 39–52 (2010).
[19] Mofid, M., Ghorbani, M. and McCabe, S.L. "On the analytical model of beam-to-column semi-rigid connections, using plate theory", *Thin-Walled Structures*, 39, pp. 307–325 (2001).
[20] CEN, EN 1993-1-8:2005, EC3: Design of Steel Structures, Part 1.8: Design of Joints (May 2005).
[21] Mohamadi-Shoore, M.R. and Mofid, M. "Basic issues in the analytical simulation of unstiffened extended end plate connection", *International Journal of Science and Technology, Scientia Iranica*, 11(4), pp. 302–311 (2004).
[22] Mofid, M., Mohamadi, M.R. and McCabe, S.L. "Analytical approach on end plate connection: ultimate and yielding moment", *Journal of Structural Engineering, ASCE*, 131(3), pp. 449–456 (2005).
[23] Mohamadi-Shoore, M.R. and Mofid, M. "Parametric analysis of steel bolted flush end plate beam splice connections using finite element modeling", *Journal of Constructional Steel Research*, (2008).
[24] AISC, Seismic provisions for structural steel buildings, American Institute of Steel Construction, Chicago (2002).
[25] Shi, Y.J., Chan, S.L. and Wong, Y.L. "Modeling for moment–rotation characteristics for end plate connections", *Journal of Structural Engineering, ASCE*, 122(11), pp. 1300–1306 (1996).
[26] Bahaari, M.R. and Sherbourne, A.N. "Finite element prediction of end plate bolted connection behavior. II: analytic formulation", *Journal of Structural Engineering, ASCE*, 123(2), pp. 165–175 (1997).
[27] Krishnamurthy, N., Huang, H.T., Jeffery, P.K. and Avery, L.K. "Analytical $M - \Phi$ curves for end plate connections", *Journal of Structural Division, ASCE*, 105(1), pp. 133–145 (1979).
[28] Tarpy, T.S. and Cardinal, J.W. "Behavior of semi-rigid beam-to-column end plate connections", *Proceeding of Conference: 'Joints in Structural Steelwork'*, pp. 2.3–2.25, Halsted Press, London (1981).

M.R. Mohamadi-Shoore graduated with B.S., M.S. and Ph.D. degrees in Civil Engineering from Sharif University of Technology, Tehran, Iran, in 2000, 2002 and 2008, respectively. At present, he is Assistant Professor in the Civil Engineering Department at the Islamic Azad University in Chalus, Iran. His research interests include seismic analysis of steel frames, focusing on the behavior of semi-rigid connections.

Massood Mofid, is a professor of Structural and Earthquake Engineering at Sharif University of Technology, Iran. He has taught and instructed Basic and Advance Engineering courses in the field of Structural Mechanics and Earthquake Engineering. His research interest is in the area of Engineering Mechanics and Structural Dynamics, Application and Implementation of Finite Element Technique in Static and Dynamic Problems with emphasis on Theory and Design.